

Accuracy of Ultrasound Imaging in the Differential Diagnosis of Inflammatory Radicular Cyst and Periapical Granuloma: A Systematic Review and Meta-Analysis of Operative Characteristics

 Nestor RIOS OSORIO,¹  Oscar JIMÉNEZ PEÑA,²  Marcela CONTRERAS IBARRA,²
 Marggie GRAJALES,³  Rafael FERNÁNDEZ GRISALES⁴

¹Biomedical Sciences PhD Programme, Universidad El Bosque, Bogotá, Colombia

²Department of Endodontics, University Institution Colegios de Colombia UNICOC, Bogotá, Colombia

³Laser Dentistry Master Programme, European Programme EMDOLA, University of Barcelona, Barcelona, Spain

⁴Department of Postgraduate Endodontics, CES University, School of Dentistry, Medellín, Colombia

ABSTRACT

This systematic review aimed to assess the accuracy of ultrasonic (US) imaging in the differential diagnosis between inflammatory radicular cysts (IRCs) and periapical granulomas (PGs) compared with the histological examination as the reference standard. Scopus, Medline (PubMed), and Web of Science were searched from inception to April 2024. The Methodological quality was assessed using the QUADAS-2 tool. Thirteen cross-sectional studies published between 2003 and 2023 were included in this study. A total sample of 275 patients (one tooth / per patient) comparing ultrasound test vs. histopathological examination was assessed. The summary measures of the US imaging test were: sensitivity= 0.96 [95% CI, 0.93–0.99], specificity= 0.83 [95% CI, 0.76–0.88], LR+ = 3.498 [95% CI, 2.079–5.885], LR- = 0.091 [95% CI, 0.050–0.164], DOR = 65.848 (95% CI, 28.857–150.25) and AUC=0.97 (95% CI, 0.95–1.00). The methodological assessment was variable in all domains and studies. Approximately 90% and 70% of the studies revealed some form of risk of bias concern in the domains -flow and timing-, and -reference standard-, respectively. US imaging can be regarded as a highly accurate and consistent method for IRC vs. PG differential diagnosis. The echotexture features of periapical lesions in US images reflected their histopathological characteristics.

Keywords: Differential diagnosis, predictive values, radicular cysts, sensitivity, specificity, ultrasound

Please cite this article as:

Rios Osorio N, Jiménez Peña O, Contreras Ibarra M, Grajales M, Fernández Grisales R. Accuracy of Ultrasound Imaging in the Differential Diagnosis of Inflammatory Radicular Cyst and Periapical Granuloma: A Systematic Review and Meta-Analysis of Operative Characteristics. *Eur Endod J* 2025; 10: 104-115

Address for correspondence:

Nestor Rios Osorio
Biomedical Sciences PhD
Programme, Universidad El
Bosque, Bogotá, Colombia
E-mail: dadopi1981@gmail.com

Received : October 02, 2024,

Revised : November 27, 2024,

Accepted : December 20, 2024

Published online: March 19, 2025
DOI 10.14744/eej.2024.84755

This work is licensed under
a Creative Commons
Attribution-NonCommercial
4.0 International License.



HIGHLIGHTS

- Preoperative diagnosis of inflammatory radicular cysts is a critical topic, since the histological nature of periapical endodontic lesions may directly influence the outcome of endodontic treatment.
- Ultrasound can provide preoperative reliable information on the pathological nature of periapical endodontic lesions through the echotexture of their contents and the presence and features of vascularity.
- Ultrasound can be regarded as a highly accurate and consistent method for inflammatory radicular cyst differential diagnosis.

INTRODUCTION

Endodontic periapical lesions can be defined as defensive, hyperplastic, and reactive lesions that result from the host's effective attempt to prevent the spread of pathogenic bacteria, mi-

crobial products, and toxins from the infected root canal into the surrounding tissues (1, 2). According to their histopathologic features, most endodontic periapical lesions can be classified as periapical granulomas (PGs) or inflamma-

tory radicular cysts (IRCs). Both PGs and IRCs manifest radiographically as periapical radiolucencies/hypodensities (1, 2). Although apical periodontitis (AP) is the clinical/radiographic diagnosis for both conditions, PG and IRC differ significantly from a histopathologic perspective (1). Consequently, PG and IRC might be considered as two different pathological entities of the same inflammatory phenomena (1, 2).

PGs are chronic inflammatory lesions, characterized by a significant infiltration of plasmatic cells, lymphocytes, multinucleated giant cells, and histiocytes, encapsulated in granulomatous tissue (1, 3). IRCs are a direct sequel of PGs. IRCs are defined as a pathological cavity lined by a stratified squamous epithelium, enclosing fluid, semifluid, or gaseous contents (1, 3, 4). Histologically, IRCs can be classified as "true" or "bay" cysts, depending on how the cyst cavity relates to the root canal through the apical foramen (5). Notably, even though PGs and IRCs are two phases from the same immune reaction and are triggered by the same antigenic stimulus, not all PGs develop into IRCs (1).

The current reference standard for differential diagnosis (DDX) of PG and IRC is the histopathological examination of biopsy tissue (1, 6). As PGs can display random outbreaks of stratified squamous epithelium, similar to the IRCs, the histopathological DDX should be ideally performed utilizing serial or step-serial sectioning of the complete lesion with the apical portion of the root adhered to it, to attain the three-dimensional information required for differentiating between the IRC and PG (1, 6).

Diagnosis of IRCs is a crucial topic considering IRCs and PGs might demand distinct therapeutic approaches, as the histopathological features of the lesion influence the outcomes of endodontic therapy (1, 7, 8). Some authors have asserted that true IRCs may only be predictably managed surgically (1, 9, 10). Accordingly, a precise preoperative diagnosis could allow for appropriate therapeutic decisions towards performing surgical approaches (1).

Non-invasive approaches including cone beam computed tomography (CBCT), ultrasound (US) imaging, and magnetic resonance imaging (MRI), have been compared with the histological examination in diagnosing the histopathological nature of endodontic lesions before intervention. Although encouraging, the findings of these research remain controversial (1).

A recent comprehensive review of the literature summarizing the accuracy of non-invasive approaches compared with the histological examination, identified the US, as one of the methods that deliver the most accurate diagnosis of the pathologic nature of endodontic lesions (1). Furthermore, MRI is associated with lengthy scan times, claustrophobia to the gantry, inapplicability in certain situations (e.g., paediatric patients, metallic implants, or cardiac pacemakers), and high costs. Similarly, the drawbacks of CBCT include ionizing radiation and ambiguity in the interpretation of greyscale values (11).

US is a real-time, non-invasive, non-ionizing imaging method based on the echo and reflection of waves off body structures. Differentiating between distinct conditions (PGs/IRCs) is made possible by the reflected waves that are captured by a transducer, based on the differences in tissue density (11).

For the DDX between PGs and IRCs, comprehension of the operating characteristics including positive predictive value (PPV), negative predictive value (NPV), sensitivity and specificity of diagnostic methods is essential and could aid the healthcare professional in proposing individualised and more predictable endodontic therapies based on the histological nature of the AP diagnosis (12). The statistical methods, necessary to identify the accuracy, as well as the correlation between a study's sensitivity and specificity with a summary receiver operating characteristic curve (SROC-curve), were previously published (2015) (13, 14). The published guide defines the threshold for defining positive versus negative test findings, which may differ between primary research, and the application of advanced statistical methods (e.g., bivariate models/hierarchical mode) (13, 14).

Given the preceding, this systematic review and meta-analysis aimed to assess the operating characteristics of US imaging compared with the histological exam of biopsy tissue to identify their accuracy level in the DDX of IRCs vs. PGs, by employing an adjusted prevalence through a detailed quantitative analysis based on predicted values that enables comparison for preoperative clinical usage.

MATERIALS AND METHODS

A comprehensive research protocol was developed and registered in the PROSPERO database (ID. CRD42023466030). We strictly followed the PRISMA statement and the Cochrane recommendations for systematic reviews of interventions (15).

PICO Question

Population: Patients seeking endodontic therapy, with a clinical/radiographic diagnosis of AP and an indication of endodontic surgical intervention.

Intervention: US for IRCs differential diagnosis.

Comparison: Histopathological examination of biopsy tissue.

Outcome: US accuracy in the DDX of IRCs compared to the histological examination of biopsy tissue (reference standard).

Focused Question

Is US imaging's accuracy in DDX of IRCs vs. PGs in human permanent teeth comparable to histological analysis of biopsy tissue in cross-sectional studies?

Inclusion Criteria

Cross-sectional studies evaluating US accuracy in the DDX of IRCs in permanent human teeth compared with histopathological examination of biopsy tissue as a reference standard. Studies including patients with a presumptive diagnosis of AP and an indication of endodontic surgical intervention or tooth extraction and performing a direct comparison between both diagnostic methods.

Exclusion Criteria

Studies that did not report true positive (TP), false positive (FP), true negative (TN), and false negative (FN) data, or when it was not possible to calculate them. Clinical studies evaluating US imaging with no reference standard, studies

that did not define the evaluation method, laboratory-based studies or animal studies, narrative reviews, case reports, and expert opinions were excluded.

Primary outcome(s): Sensitivity, specificity, PPV, NPV and SROC curve.

Secondary outcome(s): IRCs prevalence and diagnostic odds ratio (DOR).

Information sources: Descriptors in Health Sciences (DeCS), Medical subject headings (MeSH), Emtree language, and text words were applied. We searched in Web of Science, Medline (PubMed), and Scopus from inception to April 2024. The search strategy was adapted to each database. A manual search was also conducted, through references from relevant journals, conferences, Open Grey, thesis databases, Google Scholar, and ClinicalTrials.gov among others (Table 1).

Data Extraction

Initially, two researchers independently reviewed the studies based on the title and abstract. Then, they reviewed the whole text using pre-specified inclusion criteria. Disagreements were addressed by consensus, with an additional researcher making final decisions if necessary. A standardized data sheet was used to collect data in duplicate, which included: journal, authors, year, title, study design, timing, objectives, inclusion and exclusion criteria, number of included patients, outcome definition, outcomes, association measures, anatomical location of the surgical approach and funding source.

A database was created using quantitative data from the primary studies to record PPV, NPV, sensitivity, specificity and accuracy. Data for true positive (TP), false positive (FP), true negative (TN), and false negative (FN) were collected. When the data was not available, an estimation was performed: $TP = \text{sensitivity} \times \text{prevalence}$; $FP = (\text{total } n - \text{prevalence}) - TN$; $TN = \text{specificity} \times (\text{total } n - \text{prevalence})$; and $FN = \text{prevalence} - TP$ (16).

Risk of Bias and Applicability

Two researchers assessed the risk of bias and the applicability of the primary diagnostic studies using the QUADAS-2 tool (17). QUADAS-2 assessment involves four steps: In the first phase, the systematic focused question is defined and reported; in the second phase, if necessary, for a more accurate evaluation of the primary studies, a special guide is adapted or constructed from the QUADAS-2 tool; in the third phase, the flow chart published in the primary study is reviewed, or one is created if none is reported; in the fourth phase, bias and applicability are assessed through an analysis of the information reported on primary studies, which is then divided into four key domains: (i) Patient Selection, (ii) Index Test, (iii) Reference Standard and (iv) Flow and Timing. Each domain consists of two to four signalling questions with three alternative answers: "Yes," "No," and "Unclear," which are framed so that "yes" implies a low risk of bias, "no" indicates a high risk of bias, and "unclear" indicates that inadequate data was reported. Finally, the risk of bias judgment is rated as "low," "high," or "unclear." If all signalling questions for a domain

were answered "yes", the risk of bias is assessed as low. If, on the other hand, any signalling question was responded to "no", or if several questions within a domain were replied "unclear", the domain is rated as having a high risk of bias. Domains with only one signalling question identified as "unclear" are at "unclear" risk of bias (17). Applicability was assessed in the following domains: "Patient selection," "Index test," and "Reference standard." This applicability assessment is related to the focused question defined for this study and reviewed in Phase 1, and it rates the primary study's affinity with the review (focused) question. The applicability is assessed as "low", "high", or "unclear", and, similar to the risk of bias assessment, the "unclear" category is only applied when insufficient data were supplied (17).

Data Analysis/Synthesis of Results

Review Manager 5.3 (Nordic Cochrane Centre, 2014), R Version 3.6.1 -Madauni function- (Core Team, R Development) and Stata v.12.0 (Stata Corp LLC, College Station, TX, USA) were employed to perform the statistical analysis.

A bivariate model was adopted to perform a meta-analysis for observational studies involving US imaging vs. histopathology examination of biopsy tissue. The model used hierarchical methods (14), and logarithmic-type transformation to relate precision to sensitivity and specificity. The model provided data about the SROC curve (diagnostic precision metric). The SROC univariate method uses linear regression to identify a cut-off point where sensitivity and specificity are inversely proportional to test accuracy. This can be achieved by transforming the rates of true positives and false positives. The US method was analysed using a bivariate approach based on chi-square adjustment of Mahalanobis distances, spike plots, and dispersion diagrams to check for outliers using typified random effects forecasts. The assumption of normal bivariate distribution for sensitivity and specificity logit was verified. The sensitivity and specificity values were tested using a 95% confidence interval (CI).

We standardized the predictive values of all the included primary studies using the following methods to a total prevalence of 52.61 % to enable comparison: $\text{Adj. Positive predictive value} = \frac{\text{Sensitivity} \times \text{Prevalence}}{\text{Sensitivity} \times \text{Prevalence} + (1 - \text{Specificity}) \times (1 - \text{Prevalence})}$ and $\text{Adj. Negative predictive value} = \frac{\text{Specificity} \times (1 - \text{Prevalence})}{\text{Specificity} \times (1 - \text{Prevalence}) + (1 - \text{Sensitivity}) \times \text{Prevalence}}$ (12, 13).

It is essential to estimate the diagnostic odds ratio (DOR) and area under the ROC-curve (AUC) in order to comprehend the synthesis of the outcomes. This statistical index measures diagnostic accuracy by comparing the frequency of positive results in subjects with the disease under study against those without it. The index helps indicate the degree of intensity between the outcome of a test and the condition/disease. It is independent of prevalence. The range of DOR values is zero to infinity, where a greater DOR indicates a better test result. The test is useless if $DOR = 1$, which indicates that it is not discriminating. If $DOR \geq 1$, the test is more likely to be positive in affected individuals than in healthy ones (16).

TABLE 1. Search strategy translated for each database

	Search strategy translated for each database	# Studies
PUBMED MeSH terms	((Endodontics OR endodontic disease AND Inflammatory Radicular Cyst OR residual cyst OR radicular cyst OR periapical granuloma OR apical lesion AND periapical lesion AND diagnosis OR differential diagnosis) AND (CBCT AND cone beam computed tomography) AND (biopsy OR histopathology)) NOT (magnetic resonance OR MRI)	92
	((Endodontics OR endodontic disease OR Inflammatory Radicular Cyst OR residual cyst OR radicular cyst OR periapical granuloma AND apical lesion AND periapical lesion AND diagnosis AND differential diagnosis) AND (Ultrasound with colour doppler OR power doppler applications OR ultrasound) AND (biopsy OR histopathology)) NOT (magnetic resonance OR MRI)	24
	(Endodontics OR endodontic disease OR Inflammatory Radicular Cyst OR residual cyst OR radicular cyst OR periapical granuloma AND apical lesion AND periapical lesion AND diagnosis AND differential diagnosis) AND (magnetic resonance OR magnetic resonance imaging OR MRI AND histopathology OR biopsy)	54
	((Endodontics OR endodontic disease AND Inflammatory Radicular Cyst OR residual cyst OR radicular cyst OR periapical granuloma OR apical lesion AND periapical lesion AND diagnosis OR differential diagnosis) AND (Cytokine OR chemokine OR aspiration cyst fluid OR fluid OR aspiration AND panoramic radiography) AND (histopathology OR biopsy) NOT (magnetic resonance AND MRI)	12
SCOPUS keyword plus	(Endodontics OR endodontic AND disease AND inflammatory AND radicular AND cyst OR residual AND cyst OR radicular AND cyst OR periapical AND granuloma OR apical AND lesion AND periapical AND lesion AND diagnosis OR differential AND diagnosis) AND (cbct AND cone AND beam AND computed AND tomography) AND (biopsy OR histopathology) AND NOT (magnetic AND resonance OR MRI)	28
	(Endodontics OR endodontic AND disease OR inflammatory AND radicular AND cyst OR residual AND cyst OR radicular AND cyst OR periapical AND granuloma AND apical AND lesion AND periapical AND lesion AND diagnosis AND differential AND diagnosis) AND (ultrasound AND with AND colour AND doppler OR power AND doppler AND applications OR ultrasound) AND (biopsy AND histopathology) AND NOT (magnetic AND resonance OR MRI)	3
	(Endodontics OR endodontic AND disease AND inflammatory AND radicular AND cyst OR residual AND cyst OR radicular AND cyst OR periapical AND granuloma OR apical AND lesion AND periapical AND lesion AND diagnosis OR differential AND diagnosis) AND (magnetic AND resonance OR magnetic AND resonance AND imaging OR MRI AND histopathology OR biopsy)	28
	(Endodontics OR endodontic AND disease OR inflammatory AND radicular AND cyst OR residual AND cyst OR radicular AND cyst OR periapical AND granuloma AND apical AND lesion AND periapical AND lesion AND diagnosis AND differential AND diagnosis) AND (cytokine OR chemokine OR aspiration AND cyst AND fluid OR fluid OR aspiration AND panoramic AND radiography) AND (histopathology OR biopsy) AND NOT (magnetic AND resonance AND MRI)	8
	((ALL=(Endodontics OR endodontic disease AND Inflammatory Radicular Cyst OR residual cyst OR radicular cyst OR periapical granuloma OR apical lesion AND periapical lesion AND diagnosis OR differential diagnosis)) AND ALL=(CBCT AND cone beam computed tomography)) AND ALL=(biopsy OR histopathology)) NOT ALL=(magnetic resonance OR MRI)	23
ISI WEB keywords	((ALL=(Endodontics OR endodontic disease AND Inflammatory Radicular Cyst OR residual cyst OR radicular cyst OR periapical granuloma OR apical lesion AND periapical lesion AND diagnosis OR differential diagnosis)) AND ALL=(Ultrasound with colour doppler OR power doppler applications)) AND ALL=(biopsy OR histopathology)) NOT ALL=(magnetic resonance OR MRI)	115
	((ALL=(Endodontics AND endodontic disease AND Inflammatory Radicular Cyst OR residual cyst OR radicular cyst OR periapical granuloma OR apical lesion AND periapical lesion AND diagnosis OR differential diagnosis)) AND ALL=(magnetic resonance AND magnetic resonance imaging AND histopathology AND biopsy)))	58
	((ALL=(Endodontics OR endodontic disease AND Inflammatory Radicular Cyst OR residual cyst OR radicular cyst OR periapical granuloma OR apical lesion AND periapical lesion AND diagnosis AND differential diagnosis)) AND ALL=(Cytokine OR chemokine OR aspiration cyst fluid OR fluid OR aspiration AND panoramic radiography)) AND ALL=(biopsy OR histopathology)) NOT ALL=(magnetic resonance OR MRI)	28
		473

#: Number

RESULTS

Study Selection

Based on the previously described search strategy, 475 records were initially identified. After removing 64 duplicates, 411 studies (titles and abstracts) were assessed for eligibility.

Fifteen full-text articles were screened, 2 studies were excluded (18, 19). Finally, 13 cross-sectional studies underwent qualitative and quantitative synthesis (20–32) (Fig. 1).

Characteristics and Synthesis of the Evidence of the Included Studies

Thirteen cross-sectional studies published between 2003 and 2023 were included (20–32). A total sample of 365 patients (one tooth / per patient) comparing US imaging vs. histopathological examination was assessed. Thirteen samples from the Sönmez et al. (27) study, where no histopathological analysis was conducted, and 1 sample from the Das et al. (31) study, where the histopathological diagnosis was ambiguous,

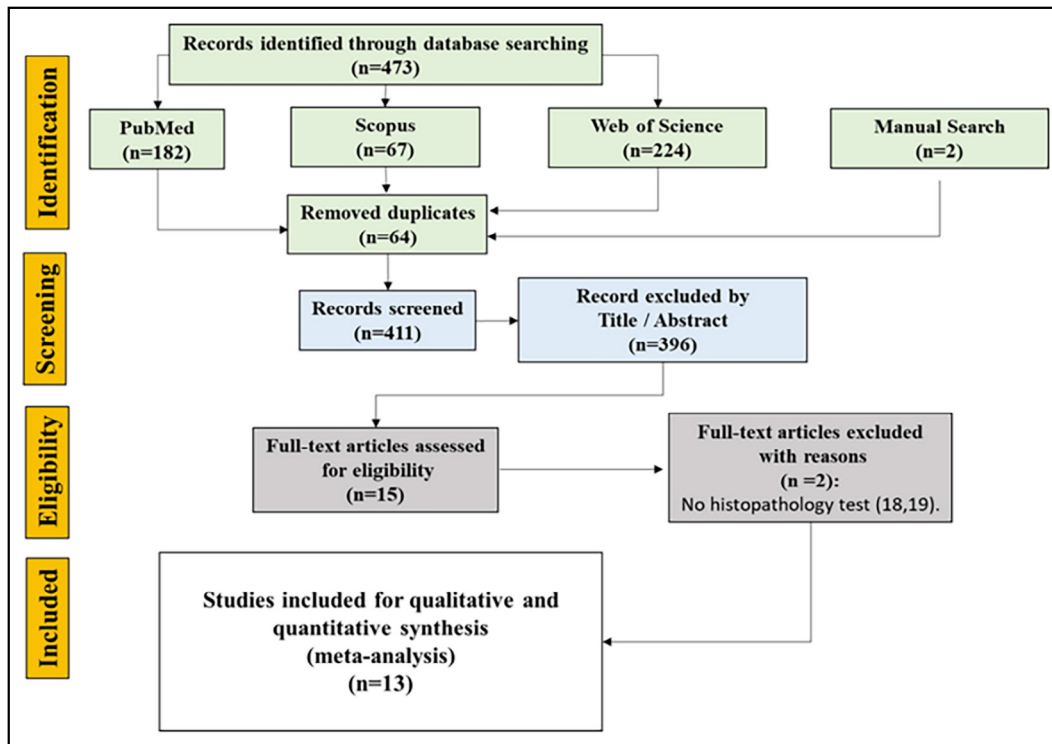


Figure 1. Flow chart of included studies, based on PRISMA 2020 guidelines

were not considered in this study (Table 2). The age range of the patients was 12 to 73 years. The included studies' sample population consisted primarily of patients scheduled for endodontic periapical surgery who were previously diagnosed with AP, based on clinical signs and symptoms, as well as bi-dimensional radiographic findings (radiolucent lesions) (20–32). Three studies also included individuals who underwent dental extraction since the treatment prognosis was deemed hopeless (22, 27, 28). US examination assessed the periapical endodontic lesions (extra-oral (transverse and longitudinal planes) and/or intraoral) employing linear and/or hockey probe transducers, operating at frequencies ranging from 7 to 15 MHz. Additionally, a colour/power Doppler examination was performed to assess the presence and features of vascularity and pulsation status of the intra-lesions (20–32).

Tikku et al. (26) examined periapical lesions in the maxilla and mandible that were located in the anterior (n=10) and posterior areas (n=20). Cotti et al. (20) in anterior (n=8) and posterior areas (n=3). Sönmez et al. (27) in anterior (n=13) and posterior areas (n=7). Jia et al. (32) in anterior (n=80) and posterior areas (n=29). Avci et al. (30) (n=10), Gundappa et al. (21) (n=15), Raghav et al. (22) (n=21), Das et al (31) (n=35), Jaswal et al. (28) (n=30) and Goel et al. (23) (n=30), only evaluated endodontic lesions located in the maxillary and mandibular anterior region. Prince et al. (24), Serindere et al. (29), and Parvathy et al. (25), did not mention the specific location of lesions assessed. A single skilled ultrasonographer carried out the US diagnosis in ten studies (20, 21, 23, 24–28, 30, 31), two ultrasonographers in one study (29), and three in two studies (22, 32). A total of 185 IRCs, and 142 PGs were diagnosed by US test and later confirmed by histopathological examination. Analysis of the 13 cross-sectional studies suggests that US can be advised

as an adjunct and useful approach for the DDX of periapical lesions (IRC/PG). US imaging can reveal reliable information on the pathogenic nature of the apical lesion which is of value in determining the treatment outcome. The echotexture properties of periapical endodontic lesions in US imaging reflected their histopathological characteristics. However, this method may be limited in its capacity to diagnose endodontic lesions in areas below dense cortical bone (22, 30, 32) (Appendix 1).

Methodological Quality

Risk of bias assessment

Only one of the thirteen included studies was rated as having a low risk of bias in all four domains assessed (32). In comparison, another study (22) was rated as having a low risk of bias in three of the four domains assessed, but the domain of "Flow and timing" was rated as having a high risk. Three studies (23–25) were assessed as having an "unclear" risk of bias in the majority of domains (Table 3).

When the evaluation was broken down by domain, the one with the most issues was "Flow and timing," considering that 12 (20–31) out of the 13 studies did not report or describe the flow chart for patient selection, nor did they describe each of the patients included in the study who were evaluated using the US test (index test) and the histopathological test. Similarly, these studies did not disclose the time period between the index and reference standard tests. The other domain whereby issues were evident in 9 (23–31) of the 13 included studies was the "Reference Standard" domain, considering these studies failed to describe how the reference standard test was performed, how it was interpreted, who interpreted it, or whether any type of blinding was implemented. In the other two domains, the majority of the studies were assessed

TABLE 2. Characterisation of study samples

Author/year	#Patients	#Observers	TP	FP	FN	TN	SE	EP	PPV (%)	NPV (%)	Adj. PPV (%)	Adj. NPV (%)
Cotti et al. (20)	11	1	6	0	1	4	85.71	100	100	80	24.28914	32.7638
Gundappa et al. (21)	15	1	7	0	0	7	100	100	100	100	24.28914	25.72112
Prince et al. (24)	15	1	12	2	0	1	100	33.33	85.71	100	58.10149	25.72112
Parvathy et al. (25)	20	1	11	0	0	9	100	100	100	100	24.28914	25.72112
Tikku et al. (26)	30	1	3	7	0	20	100	74.07	30	100	37.43979	25.72112
Sönmez et al. (27)	20	1	12	3	0	5	100	62.5	80	100	43.30763	25.72112
Jaswal et al. (28)	30	1	12	0	0	18	100	100	100	100	24.28914	25.72112
Serindere et al. (29)	20	2	14	2	1	3	93.33	60	87.5	75	44.57553	29.00836
Avci et al. (30)	10	1	8	1	1	0	88.89	0	88.89	0	75.00513	-
Das et al. (31)	34	1	25	4	0	5	100	55.56	86.21	100	46.82732	25.72112
Jia et al. (32)	109	3	44	10	2	53	95.65	84.13	81.48	96.36	32.33776	27.86497

#: Number; TP: True positive; FP: False positive; FN: False negative; TN: True negative; SE: Sensitivity; EP: Specificity; Adj.: Adjusted; PPV: Positive predictive value; NPV: Negative predictive value

as having a low risk of bias. In the "Patient Selection" domain, the few studies (20, 21, 23–25) that were classified as having an "unclear" risk of bias were related to unclear patient selection methods (inclusion criteria). In the "Index Test" domain, the few studies (23–25, 29) that were rated as having an "unclear" risk of bias did not disclose who interpreted the tests or whether any blinding was performed (Fig. 2a), (Table 3).

Applicability assessment

In the applicability analysis, almost all studies (20–23, 26–32) were identified as having a low risk of bias in the three domains reviewed ("Patient Selection"; "Index Test"; and "Reference Standard"). Two of the studies (24, 25) were classified as having an "unclear" risk of bias in the "Patient Selection" domain since the studies did not provide a detailed description of the included patients in terms of previous tests, the severity of the target condition, demographic characteristics, and any evidence of DDX or comorbidity (Fig. 2b), (Table 3).

Quantitative Analysis

Sensitivity and specificity

The pooled estimate for sensitivity and specificity of US imaging to differentially diagnose IRCs were 0.97 with 95% CI (0.93–0.99) and 0.83 with 95% CI (0.76–0.88) respectively (Fig. 3).

Predictive value analysis

The PPV and NPV values were not used for comparisons, because the disease's prevalence varies across studies and impacts the outcomes. Therefore, the positive and negative prevalence values were computed using the overall IRC prevalence (52.61%), which considers all positive results for the disease across the total sample that was assessed in all the included cross-sectional studies. Based on the adjusted prevalence report, US imaging displays a high PPV and NPV, indicating that a positive result from a US imaging test may suggest a high certainty of being an IRC. Furthermore, the Summary positive and negative likelihood ratios suggest a high probability of US identifying IRCs (Fig. 4a, b), (Table 4).

Analysis using DOR

US imaging showed a high DOR for correctly indicating a diagnosis of IRC, DOR = 65.848 (95% CI, 28.857–150.25) (Fig. 5).

AUC evaluation

As a general indicator of test performance, the area under the curve (AUC) was employed to summarise the meta-analysis's findings (AUC identifies the test's inherent capacity to distinguish between disease and healthy populations (accuracy)). The US imaging showed a high sensitivity and an FP low rate, with an AUC = 0.97 (95% CI, 0.95–1.00) (Fig. 6).

DISCUSSION

This Systematic review assessed the sensitivity, specificity, adjusted PPV, adjusted NPV, positive likelihood ratio (LR+), and negative likelihood ratio (LR-) of US imaging for the DDX of IRCs. Findings of this study (Sensitivity= 0.96 [95% CI, 0.93–0.99], specificity= 0.83 [95% CI, 0.76–0.88], LR+ = 3.498 [95% CI, 2.079–885], LR- = 0.091 [95% CI, 0.050–0.164], DOR = 65.848 (95% CI, 28.857 – 150.25) and AUC = 0.97 (95% CI, 0.95–1.00)), suggest that US can be regarded as a highly accu-

TABLE 3. Methodological quality graph of included studies (Quadas-2)

Study	Risk of bias				Applicability concerns		
	Patient selection	Index test	Reference standard	Flow and timing	Patient selection	Index test	Reference standard
Cotti et al. (20)	?	⊕	⊕	?	⊕	⊕	⊕
Gundappa et al. (21)	?	⊕	⊕	?	⊕	⊕	⊕
Raghav et al. (22)	⊕	⊕	⊕	⊗	⊕	⊕	⊕
Goel et al. (23)	?	?	?	?	⊕	⊕	⊕
Prince et al. (24)	?	?	?	⊗	?	⊕	⊕
Parvathy et al. (25)	?	?	?	⊗	?	⊕	⊕
Tikku et al. (26)	⊕	⊕	?	⊗	⊕	⊕	⊕
Sönmez et al. (27)	⊕	⊕	?	⊗	⊕	⊕	⊕
Jaswal et al. (28)	⊕	⊕	?	⊗	⊕	⊕	⊕
Serindere et al. (29)	⊕	?	?	⊗	⊕	⊕	⊕
Avci et al. (30)	⊕	⊕	?	⊗	⊕	⊕	⊕
Das et al. (31)	⊕	⊕	?	⊗	⊕	⊕	⊕
Jia et al. (32)	⊕	⊕	⊕	⊕	⊕	⊕	⊕

⊕=Low risk, ?=Unclear risk, ⊗=High risk

TABLE 4. Grouped estimates of sensitivity, specificity, predictive values, LR+, LR- and AUC of ultrasound test

SE [95% CI]	EP [95% CI]	LR+ [95% CI]	LR- [95% CI]	Adj. PPV	Adj. NPV	AUC [95% CI]
0.96 [0.93–0.99]	0.83 [0.76–0.88]	3.498 [2.079–5.885]	0.091 [0.050–0.164]	0.86 [0.81–0.91]	0.93 [0.88–0.97]	0.97 [0.95–1.00]

LR+: Positive likelihood ratio, LR-: Negative likelihood ratio, SE: Sensitivity, EP: Specificity, Adj.: Adjusted, PPV: Positive predictive value, NPV: Negative predictive value, AUC: Area under the ROC curve, CI: Confidence interval

rate and consistent method for IRC DDX. The US can offer accurate details on the pathological nature of periapical endodontic lesions through the echotexture of their contents as well as the existence and features of vascularity. Notably, the included observational studies showed moderate heterogeneity (I²=63.6%). The spread and skewness of the data, visualized in the Summary receiver operating characteristic (SROC) plot may contribute to the considerable heterogeneity (Fig. 6).

Since each primary study's evaluation was conducted with a different prevalence, the studies' results were inconsistent. Therefore, the PPV and NPV were adjusted to a standard prevalence (52.61%).

Overall, it can be estimated that this systematic review has a moderate risk of bias (QUADAS-2). Mainly because less than 10% of the studies presented a low risk of bias in the -flow and timing- domain. Most studies fail to provide a flow chart of patient selection and do not describe the time elapsed between the US and histopathological test. Similarly, less than 30% of the studies represented a low risk of bias in the -reference standard- domain. Very few studies described who performed the standard test, under what settings, and whether they were subjected to any test-specific blinding. As a result, the findings drawn by these studies regarding the test's accuracy are subjective (Table 3) (Fig. 2a).

Sound is mechanical energy that flows through a medium by alternating high- and low-pressure waves (33). Clinical US imaging involves sound waves-living tissue interactions to generate images of the target tissues or, in Doppler-based formats, deter-

mine the rate of moving tissue, usually blood flow. US stands for sound waves with a frequency above 20,000 cycles per second (Hz). Diagnostic ultrasonography often employs frequencies ranging from 2 to 15 MHz (106 cycles/second). Sound waves propagate across soft tissues at these frequencies, based on their acoustic impedance. The specific tissue's acoustic impedance is governed by its transmission velocity and density. The vast majority of soft tissues and blood display a transmission speed of around 1540 m/sec (33, 34). Hence, density primarily governs the acoustic impedance of the majority of soft tissues. When two tissues of differing densities are located adjacent, an acoustic impedance mismatch occurs, and sound waves are reflected by the mismatch (33, 34). The larger the acoustic mismatch, the more sound waves are reflected and returned to the transducer (the transducer generates sound waves and receives reflected sound waves). Areas with substantial tissue density variations, and consequently more reflected sound waves, are typically perceived as brighter areas on the US image (34, 35). US imaging is most suitable for soft tissue screening, and it is frequently hindered by bone and gas-filled structures. Sound travels swiftly through bone structures. In contrast, sound conducts deficiently across the air and air-filled structures. The huge acoustic impedance mismatch between bone and gas interfaces and soft tissue leads most of the waves to be reflected. High reflectivity inhibits sound wave propagation into deeper tissues and may cause generate artifacts in the final US image (34, 35).

Differentiating between IRCs and PGs in the US evaluation is dependent on several parameters. IRCs typically present as hypoechoic or anechoic lesions with a well-defined contour and

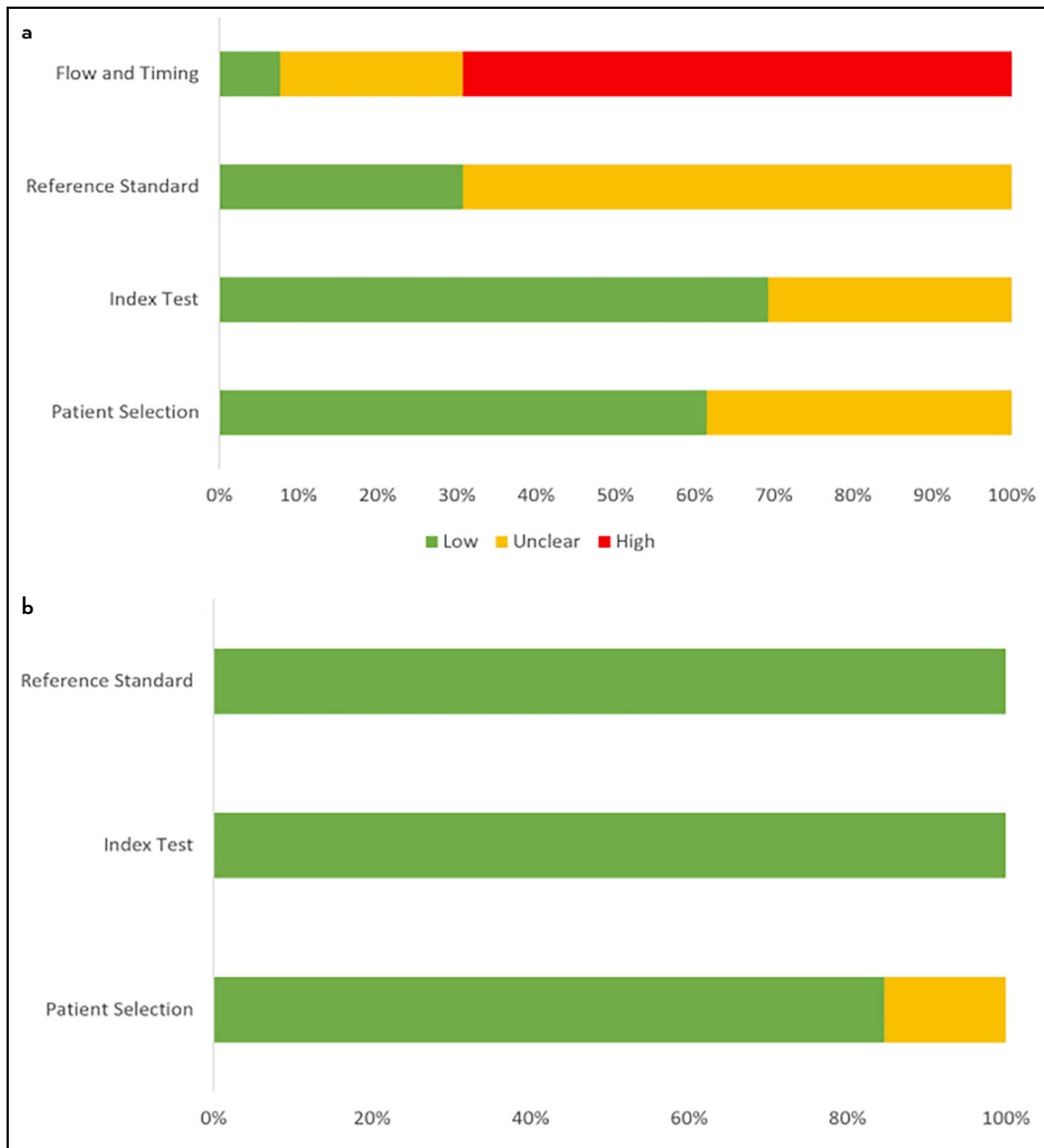


Figure 2. (a) Proportion of studies with low, high, or unclear risk of bias (%). (b) Proportion of studies with low, high, or unclear concerns regarding applicability (%)

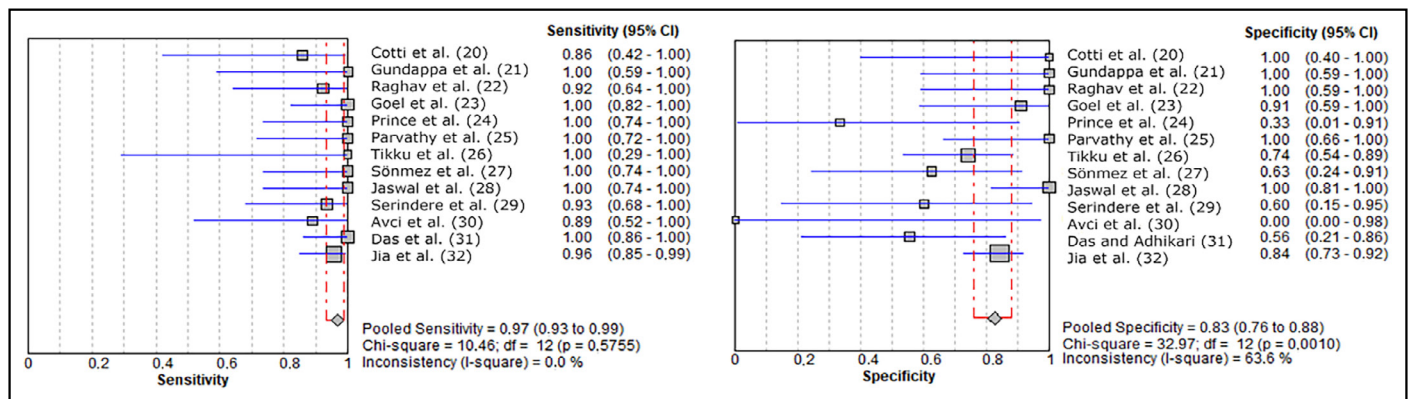


Figure 3. Forest plot of ultrasound test

CI: Confidence interval

smooth margins, indicating the presence of clear fluid content without evidence of internal vascularisation on the application of both colour Doppler and power Doppler. The anechoic

is caused by the cysts being filled with fluid rather than solid or inflammatory components, resulting in a homogeneous US image (20, 23). PGs exhibit varying echogenicity, ranging from

a	Study	LR-	[95% Conf. Interval.]	% Weight
	Cotti et al. (20)	0.208	0.048 - 0.908	16.13
	Gundappa et al. (21)	0.067	0.005 - 0.982	4.83
	Raghav et al. (22)	0.114	0.025 - 0.524	15.07
	Goel et al. (23)	0.029	0.002 - 0.445	4.64
	Prince et al. (24)	0.103	0.005 - 2.056	3.89
	Parvathy et al. (25)	0.044	0.003 - 0.664	4.73
	Tikku et al. (26)	0.171	0.013 - 2.304	5.16
	Sönmez et al. (27)	0.063	0.004 - 1.002	4.56
	Jaswal et al. (28)	0.040	0.003 - 0.599	4.73
	Serindere et al. (29)	0.111	0.015 - 0.841	8.53
	Avci et al. (30)	0.600	0.036 - 10.042	4.40
	Das et al. (31)	0.035	0.002 - 0.576	4.45
	Jia et al. (32)	0.052	0.013 - 0.201	18.90
	(REM) pooled LR-	0.091	0.050 - 0.164	
Heterogeneity chi-squared = 6.58 (d.f.= 12) p = 0.884				
Inconsistency (I-square) = 0.0 %				
Estimate of between-study variance (Tau-squared) = 0.0000				
No. studies = 13.				
b	Study	LR+	[95% Conf. Interval.]	% Weight
	Cotti et al. (20)	8.125	0.574 - 115.07	3.07
	Gundappa et al. (21)	15.000	1.018 - 220.92	3.00
	Raghav et al. (22)	14.286	0.970 - 210.44	3.00
	Goel et al. (23)	7.800	1.743 - 34.908	6.69
	Prince et al. (24)	1.538	0.715 - 3.312	11.32
	Parvathy et al. (25)	19.167	1.283 - 286.40	2.97
	Tikku et al. (26)	3.267	1.597 - 6.682	11.69
	Sönmez et al. (27)	2.473	1.082 - 5.649	10.89
	Jaswal et al. (28)	36.538	2.366 - 564.32	2.91
	Serindere et al. (29)	2.333	0.791 - 6.885	9.10
	Avci et al. (30)	1.133	0.489 - 2.629	10.78
	Das et al. (31)	2.179	1.096 - 4.334	11.89
	Jia et al. (32)	6.026	3.402 - 10.675	12.70
	(REM) pooled LR+	3.498	2.079 - 5.885	
Heterogeneity chi-squared = 33.33 (d.f.= 12) p = 0.001				
Inconsistency (I-square) = 64.0 %				
Estimate of between-study variance (Tau-squared) = 0.4698				
No. studies = 13.				

Figure 4. (a) Summary negative likelihood ratio (random effects model). (b) Summary positive likelihood ratio (random effects model)

LR: Likelihood ratio, REM: Random effects model

	Study	DOR	[95% Conf. Interval.]	% Weight
	Cotti et al. (20)	39.000	1.277 - 1190.9	5.82
	Gundappa et al. (21)	225.00	3.926 - 12895.0	4.15
	Raghav et al. (22)	125.00	4.491 - 3479.0	6.15
	Goel et al. (23)	273.00	10.197 - 7308.9	6.30
	Prince et al. (24)	15.000	0.464 - 485.32	5.63
	Parvathy et al. (25)	437.00	7.900 - 24172.1	4.23
	Tikku et al. (26)	19.133	0.880 - 415.89	7.18
	Sönmez et al. (27)	39.286	1.720 - 897.10	6.95
	Jaswal et al. (28)	925.00	17.197 - 49755.6	4.29
	Serindere et al. (29)	21.000	1.404 - 314.05	9.30
	Avci et al. (30)	1.889	0.050 - 72.023	5.13
	Das et al. (31)	62.333	2.912 - 1334.2	7.25
	Jia et al. (32)	116.60	24.260 - 560.42	27.61
	(REM) pooled DOR	65.848	28.857 - 150.25	
Heterogeneity chi-squared = 10.12 (d.f.= 12) p = 0.606				
Inconsistency (I-square) = 0.0 %				
Estimate of between-study variance (Tau-squared) = 0.0000				
No. studies = 13.				

Figure 5. Summary diagnostic odds ratio (random effects model)

DOR: Diagnostic odds ratio

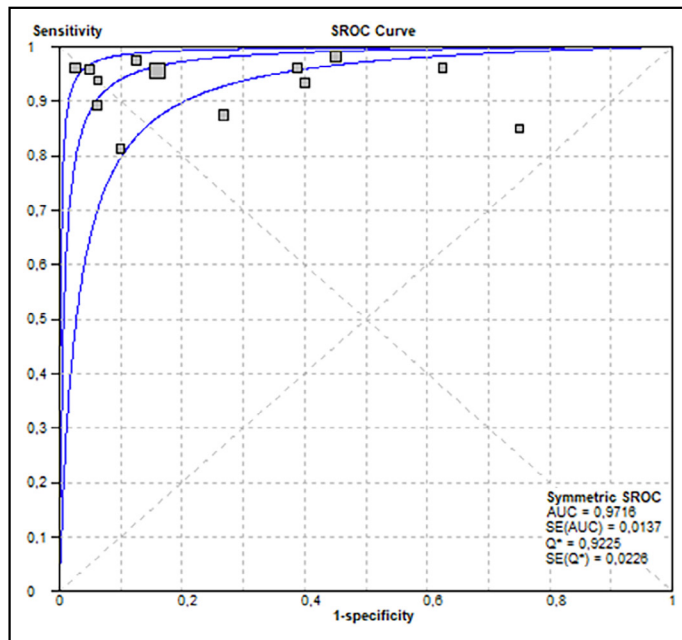


Figure 6. Summary receiver operating characteristic (SROC) plot for the ultrasound test. Summary ROC curves (solid lines). Every square represents the sensitivity and specificity estimate from one study, and the size of the square reflects the sample size.

*: The point of the curve in which sensitivity equals specificity. SE: Standard error, AUC: Area under the curve

hypochoic (in the core) to hyperechoic (in the periphery). PGs describe uneven patterns at their margins (irregular walls), indicating inflammatory tissue infiltration, which suggests a more aggressive and less defined inflammatory phenomenon (20,23). PGs exhibit a rich vascular supply on colour and power Doppler evaluation (20, 23). To properly interpret IRCs using US imaging, the equipment must have high-frequency transducers, particularly in the 7 to 12 MHz range. This high frequency is required to obtain optimal spatial resolution (1, 32).

The current study's findings are consistent with those of two previously published comparable systematic reviews (11, 36). The systematic review by Musu et al. (36) found that US imaging is effective for diagnosing infective and inflammatory periapical lesions, cysts, non-odontogenic tumours, odontogenic tumours, arteriovenous malformations, and endodontic lesions when compared to histological analysis (36). However, unlike the present study, the Musu et al. (36) study, included case reports or case series instead of cross-sectional studies, assessed the quality of the included studies using a modified Cochrane Collaboration's tools rather than the QUADAS-2 tool and did not perform quantitative analysis, which could raise the possibility of bias when presenting the results. The systematic review by Natanasabapathy et al. (11) found estimations of US's sensitivity and specificity to diagnose IRCs of 0.98 and 0.99 respectively, and an AUC of 0.99, which suggests that US is a reliable tool in DDX of IRCs. Notably, all the included studies had inherent publication bias (11). Unlike the study by Natanasabapathy et al. (11), the present study employs an adjusted prevalence (the PPV and the NPVs were calculated with the total IRC prevalence) which allows a more precise comparison between studies and reduces the variance of prevalence estimators.

However, it is also worth noting that there are several drawbacks inherent in the nature of US that must be addressed when performing the DDX of the IRC. First and foremost, a thorough understanding of the device's functionality and underlying systems is required for optimal image adjustment and documentation. Likewise, it's important to receive proper training in interpreting US images. Setzer et al. (37) demonstrated that a convolutional artificial intelligence approach accurately detects periapical lesions in CBCT images. A similar approach may eliminate operator or subjective bias when assessing US images. Although periapical lesion size has been proposed to provide insight into the nature of the underlying pathologic process, US-based size estimations in three dimensions are unreliable. The bony borders of the lesions may create an acoustic shadow on the lateral walls, making it difficult to accurately measure with electronic callipers (21). The inability of US to analyse deep intrabony periapical lesions—where the endodontic lesion is covered in a thick layer of cortical bone—has also been documented (11, 22, 30, 32). This constraint is mirrored in the nature of most included studies' samples, which choose to analyse only teeth in the anterior region, where the bone cortical is thinner, thus introducing selection bias and limiting the generalizability of the findings to posterior teeth or thicker bone areas. In the study by Tikku et al. (26), a correlation was found between bone thickness and lesion detection ($p=0.033$). All patients with cortical bone thickness less than 1.6 mm (mean value) were accurately diagnosed, whereas only 65% of those with bone thickness ≥ 1.6 mm turned out to have a lesion (26). Similarly, Jia et al. (32) reported that in two cases, the US-test diagnosed PGs were histopathologically confirmed to be IRCs. Both samples featured posterior areas, where bone thickness and continuity could have led to the misdiagnosis. The bone's acoustic impedance leads the lesion margins to seem poorly defined on US images, leading to a misdiagnosis of PG (32). US waves are thought to be inhibited by intact cortical bone. However, it has also been argued that an interruption in the cortical plate is not necessary to visualize a periapical lesion, since a thinning of the cortical may be enough to provide an acoustic window for the ultrasonic waves to reach the bone defect (38). Notably, Musu et al. (38), used an *ex vivo* model to demonstrate that artificial bony lesions in bovine mandible bones may be reliably detected with US imaging, regardless of diameter, thickness, or cortical plate perforation. Finally, the inability to distinguish between a true and bay cyst and the unavailability of specifically made probes that can be utilized in every area of the oral cavity are technical barriers to employing US for IRC diagnosis (11). The PRISMA Declaration and the Cochrane Collaboration were strictly adhered to in the present study. However, the results' considerable heterogeneity makes interpretation problematic. Furthermore, the sampling error in the estimated between-study variance and the observed within-study variances may be large when the sample sizes are small, as is the case for the majority of the studies included in this systematic review. As a result, the coverage probability may be much lower than the nominal level and the overall estimate's confidence interval (CI) may be poor (39). Consequently, reducing bias requires a robust sample size, a clearly and well-defined study design and multiple blinded calibrated ultrasonographers/endodontists.

CONCLUSION

US imaging can be regarded as a highly accurate and consistent method for IRC differential diagnosis. US offers reliable details on the pathological nature of periapical endodontic lesions through the echotexture of their contents and the existence and features of vascularity. However, it should be highlighted that the results herein reported are primarily based on samples acquired from anterior teeth/areas, due to the apparent limits imposed by thick bone corticals in posterior teeth/areas, particularly at the mandibular level. The results of this study must be interpreted with caution, as 12 out of the 13 included observational studies raised concerns about the potential risk of bias. Finally, it is recommended that diagnostic studies report all the most relevant operating characteristics.

Disclosures

Appendix file: [https://jag.journalagent.com/eurendodj/abs_files/EEJ-84755/EEJ-84755_\(0\)_EEJ-2024-09-150_Appendix.pdf](https://jag.journalagent.com/eurendodj/abs_files/EEJ-84755/EEJ-84755_(0)_EEJ-2024-09-150_Appendix.pdf)

Authorship Contributions: Concept – N.R.O., M.C.I.; Design – N.R.O., O.J.P.; Supervision – N.R.O.; Funding – N.R.O., R.F.G.; Data collection and/or processing – N.R.O., M.C.I.; Data analysis and/or interpretation – O.J.P.; Literature search – N.R.O.; Writing – N.R.O., M.G.; Critical review – M.G., R.F.G., M.C.I.

Conflict of Interest: All authors declared no conflict of interest.

Use of AI for Writing Assistance: The authors declared that they did not use any type of artificial intelligence (AI), or any kind of assisted technologies to conduct this systematic review and meta-analysis.

Financial Disclosure: The authors declared that this study received no financial support.

Peer-review: Externally peer-reviewed.

REFERENCES

- Rios Osorio N, Caviedes-Bucheli J, Mosquera-Guevara L, Adames-Martinez JS, Gomez-Pinto D, Jimenez-Jimenez K, et al. The paradigm of the inflammatory radicular cyst: biological aspects to be considered. *Eur Endod J* 2023; 8(1):20–36. [CrossRef]
- Karamifar K, Tondari A, Saghiri MA. Endodontic periapical lesion: an overview on the etiology, diagnosis and current treatment modalities. *Eur Endod J* 2020; 5(2):54–67. [CrossRef]
- García CC, Sempere FV, Diago MP, Bowen EM. The post-endodontic periapical lesion: histologic and etiopathogenic aspects. *Med Oral Patol Oral Cir Bucal* 2007; 12(8):E585–90.
- Schulz M, von Arx T, Altermatt HJ, Bosshardt D. Histology of periapical lesions obtained during apical surgery. *J Endod* 2009; 35(5):634–42. [CrossRef]
- Ricucci D, Rôças IN, Hernández S, Siqueira JF Jr. "True" versus "Bay" apical cysts: clinical, radiographic, histopathologic, and histobacteriologic features. *J Endod* 2020; 46(9):1217–27. [CrossRef]
- Çalışkan MK, Kaval ME, Tekin U, Ünal T. Radiographic and histological evaluation of persistent periapical lesions associated with endodontic failures after apical microsurgery. *Int Endod J* 2016; 49(11):1011–9. [CrossRef]
- Chanani A, Adhikari HD. Reliability of cone beam computed tomography as a biopsy-independent tool in differential diagnosis of periapical cysts and granulomas: an *in vivo* study. *J Conserv Dent* 2017; 20(5):326–31. [CrossRef]
- AlMadi DM, Al-Hadlaq MA, AlOtaibi O, Alshagroud RS, Al-Ekrish AA. Accuracy of mean grey density values obtained with small field of view cone beam computed tomography in differentiation between periapical cystic and solid lesions. *Int Endod J* 2020; 53(10):1318–26. [CrossRef]
- Lin LM, Ricucci D, Lin J, Rosenberg PA. Nonsurgical root canal therapy of large cyst-like inflammatory periapical lesions and inflammatory apical cysts. *J Endod* 2009; 35(5):607–15. [CrossRef]
- Ramachandran Nair PN, Pajarola G, Schroeder HE. Types and incidence of human periapical lesions obtained with extracted teeth. *Oral Surg Oral Med Oral Pathol Oral Radiol Endod* 1996; 81(1):93–102. [CrossRef]
- Natanasabapathy V, Arul B, Mishra A, Varghese A, Padmanaban S, Elango S, et al. Ultrasound imaging for the differential diagnosis of periapical lesions of endodontic origin in comparison with histopathology - a systematic review and meta-analysis. *Int Endod J* 2021; 54(5):693–711. [CrossRef]
- Altman DG, Bland JM. Diagnostic tests 2: predictive values. *BMJ* 1994; 309(6947):102. [CrossRef]
- Kim KW, Lee J, Choi SH, Huh J, Park SH. Systematic review and meta-analysis of studies evaluating diagnostic test accuracy: a practical review for clinical researchers-part I. General guidance and tips. *Korean J Radiol* 2015; 16(6):1175–87. [CrossRef]
- Lee J, Kim KW, Choi SH, Huh J, Park SH. Systematic review and meta-analysis of studies evaluating diagnostic test accuracy: a practical review for clinical researchers-part II. Statistical methods of meta-analysis. *Korean J Radiol* 2015; 16(6):1188–96. [CrossRef]
- Urrútia G, Bonfill X. PRISMA declaration: a proposal to improve the publication of systematic reviews and meta-analyses. *Med Clin (Barc)* [Article in Spanish] 2010; 135(11):507–11. [CrossRef]
- Buenahora MR, Peraza LA, Díaz-Báez D, Bustillo J, Santacruz I, Trujillo TG, et al. Diagnostic accuracy of clinical visualization and light-based tests in precancerous and cancerous lesions of the oral cavity and oropharynx: a systematic review and meta-analysis. *Clin Oral Investig* 2021; 25(6):4145–59. [CrossRef]
- Whiting PF, Rutjes AW, Westwood ME, Mallett S, Deeks JJ, Reitsma JB, et al. QUADAS-2 Group. QUADAS-2: a revised tool for the quality assessment of diagnostic accuracy studies. *Ann Intern Med* 2011; 155(8):529–36. [CrossRef]
- Cotti E, Campisi G, Garau V, Puddu G. A new technique for the study of periapical bone lesions: ultrasound real time imaging. *Int Endod J* 2002; 35(2):148–52. [CrossRef]
- Aggarwal V, Singla M. Use of computed tomography scans and ultrasound in differential diagnosis and evaluation of nonsurgical management of periapical lesions. *Oral Surg Oral Med Oral Pathol Oral Radiol Endod* 2010; 109(6):917–23. [CrossRef]
- Cotti E, Campisi G, Ambu R, Dettori C. Ultrasound real-time imaging in the differential diagnosis of periapical lesions. *Int Endod J* 2003; 36(8):556–63. [CrossRef]
- Gundappa M, Ng SY, Whites EJ. Comparison of ultrasound, digital and conventional radiography in differentiating periapical lesions. *Dentomaxillofac Radiol* 2006; 35(5):326–33. [CrossRef]
- Raghav N, Reddy SS, Giridhar AG, Murthy S, Yashodha Devi BK, Santana N, et al. Comparison of the efficacy of conventional radiography, digital radiography, and ultrasound in diagnosing periapical lesions. *Oral Surg Oral Med Oral Pathol Oral Radiol Endod* 2010; 110(3):379–85. [CrossRef]
- Goel S, Nagendrareddy SG, Raju MS, Krishnojiroo DR, Rastogi R, Mohan RP, et al. Ultrasonography with color Doppler and power Doppler in the diagnosis of periapical lesions. *Indian J Radiol Imaging* 2011; 21(4):279–83. [CrossRef]
- Prince CN, Annapurna CS, Sivaraj S, Ali IM. Ultrasound imaging in the diagnosis of periapical lesions. *J Pharm Bioallied Sci* 2012; 4(Suppl 2):S369–72. [CrossRef]
- Parvathy V, Kumar R, James EP, George S. Ultrasound imaging versus conventional histopathology in diagnosis of periapical lesions of endodontic origin: a comparative evaluation. *Indian J Dent Res* 2014; 25(1):54–7. [CrossRef]
- Tikku AP, Bharti R, Sharma N, Chandra A, Kumar A, Kumar S. Role of ultrasound and color doppler in diagnosis of periapical lesions of endodontic origin at varying bone thickness. *J Conserv Dent* 2016; 19(2):147–51. [CrossRef]
- Sönmez G, Kamburoğlu K, Yılmaz F, Koç C, Barış E, Tüzüner A. Versatility of high resolution ultrasonography in the assessment of granulomas and radicular cysts: a comparative *in vivo* study. *Dentomaxillofac Radiol* 2019; 48(6):20190082. [CrossRef]
- Jaswal S, Patil N, Singh MP, Dadarwal A, Sharma V, Sharma AK. A comparative evaluation of digital radiography and ultrasound imaging to detect periapical lesions in the oral cavity. *Cureus* 2022; 14(10):e30070. [CrossRef]

29. Serindere G, Aktuna Belgin C, Bulte M, Gursoy D, Salimov F. Comparison of ultrasonography and cone beam computed tomography in the differential diagnosis of periapical lesions: a prospective radiopathological study. *J Dent Indones* 2022; 29(3):194–201. [\[CrossRef\]](#)
30. Avci F, Etöz M, Üstün Y, Arslan T. Evaluation of ultrasonography as a diagnostic tool in the management of periapical cysts and granulomas: a clinical study. *Imaging Sci Dent* 2022; 52(2):209–17. [\[CrossRef\]](#)
31. Das S, Adhikari HD. Reliability of ultrasonography in differentially diagnosing periapical lesions of endodontic origin in comparison with Intra-oral periapical radiography and cone-beam computed tomography: an *in vivo* study. *J Conserv Dent* 2021; 24(5):445–50. [\[CrossRef\]](#)
32. Jia W, Jing H, Xia G, Angang D, Wei Z, Pengfei Z, et al. Utility of ultrasonography for diagnosing and differentiating periapical granuloma from radicular cyst. *Acad Radiol* 2023; 30(10):2329–39. [\[CrossRef\]](#)
33. Curriculum for Fundamentals of Ultrasound in Clinical Practice. *J Ultrasound Med* 2019; 38(8):1937–50. [\[CrossRef\]](#)
34. Coatney RW. Ultrasound imaging: principles and applications in rodent research. *ILAR J* 2001; 42(3):233–47. [\[CrossRef\]](#)
35. Seidel G, Algermissen C, Christoph A, Katzer T, Kaps M. Visualization of brain perfusion with harmonic gray scale and power doppler technology: an animal pilot study. *Stroke* 2000; 31(7):1728–34. [\[CrossRef\]](#)
36. Musu D, Rossi-Fedele G, Campisi G, Cotti E. Ultrasonography in the diagnosis of bone lesions of the jaws: a systematic review. *Oral Surg Oral Med Oral Pathol Oral Radiol* 2016; 122(1):e19–29. [\[CrossRef\]](#)
37. Setzer FC, Shi KJ, Zhang Z, Yan H, Yoon H, Mupparapu M, et al. Artificial intelligence for the computer-aided detection of periapical lesions in cone-beam computed tomographic images. *J Endod* 2020; 46(7):987–93. [\[CrossRef\]](#)
38. Musu D, Cadeddu Dessalvi C, Shemesh H, Frenda MG, Mercurio G, Cotti E. Ultrasound examination for the detection of simulated periapical bone lesions in bovine mandibles: an *ex vivo* study. *Int Endod J* 2020; 53(9):1289–98. [\[CrossRef\]](#)
39. Lin L. Bias caused by sampling error in meta-analysis with small sample sizes. *PLoS One* 2018; 13(9):e0204056. [\[CrossRef\]](#)